Fast Time-resolved Mid-infrared Spectroscopy Using an Interferometer

Gregory D. Smith and Richard A. Palmer
Duke University, Durham, NC, USA

1 INTRODUCTION

The development of fast time-resolved mid-infrared (MIR) spectroscopy since the 1980s has provided an effective tool for the study of transient chemical species in dynamic systems.[1,2] Interest in this particular spectroscopy stems from the virtual universality of infrared (IR) absorption, the rich molecular structural information contained in the MIR spectrum, and the fast time scale of vibrational motions [compared, for example, with the nuclear magnetic resonance (NMR) time scale]. The incorporation of an interferometric spectrometer in these time-resolved studies allows multiple vibrational frequencies to be monitored simultaneously across a wide spectral window. With this tool, the processes of ligand binding and dissociation, protein folding, photocycles, reaction kinetics, and excited-state electronic structures, as well as a host of other dynamic chemical phenomena, can all be measured and characterized. Over the years, efforts in this area have centered on increasing the speed at which broadband, high-resolution spectra can be collected.[1,3–5]

Time-resolved MIR spectroscopic studies of transient species have been conducted over a temporal range stretching from minutes to femtoseconds. Figure 1 shows that each time regime along that scale has come to be dominated by a specific time-resolved infrared (TRIR) technique, that a considerable overlap exists at the boundaries, and that interferometric techniques dominate a large portion of the dynamic spectrum. The superiority of each technique in a particular time regime can be ascribed to that technique's maximum time resolution, sensitivity, spectral range, cost, and ease of use.

Although several laser-based approaches to TRIR, both single-frequency and continuum-generation methods, offer extremely high time resolution, Fourier transform interferometric time-resolved infrared (FT-TRIR) techniques have distinct advantages over both these methods in terms of spectral bandwidth, resolution, and sensitivity. The use of an interferometer to encode the spectral characteristics also brings a wide array of added benefits to TRIR experiments. Fourier transform infrared (FT-IR) spectroscopy's well-known multiplex (Fellgett), throughput (Jacquinot), and registration (Connes) advantages, which have led to the almost total replacement of dispersive instruments for static measurements, also persist in time-resolved spectroscopy (TRS) applications. The rise time of practical broadband MIR detectors is currently limited to $\sim$1 ns, and therefore, the fastest FT-TRIR technique as currently demonstrated has its upper limit in that time regime.[3] However, the pulsed-asynchronous sampling technique (see below and Volume 1, Part 2) promises to extend that limit by several orders of magnitude, thus pressing laser-based techniques even further in their most advantageous area, namely time resolution.

Despite the present temporal limitation of FT-IR, the advantages provided by interferometric spectral encoding make it superior to dispersive and laser-based methods for producing fast time-resolved, high spectral resolution measurements in which the resulting spectra cover the entire MIR region. The chief drawbacks of the latter techniques, and consequently the areas where Fourier transform (FT)-based methods excel, include the limited tunability of probe lasers (both in range and resolution), the complexity of multicomponent laser systems, and the expense of the

© John Wiley & Sons Ltd, 2002.

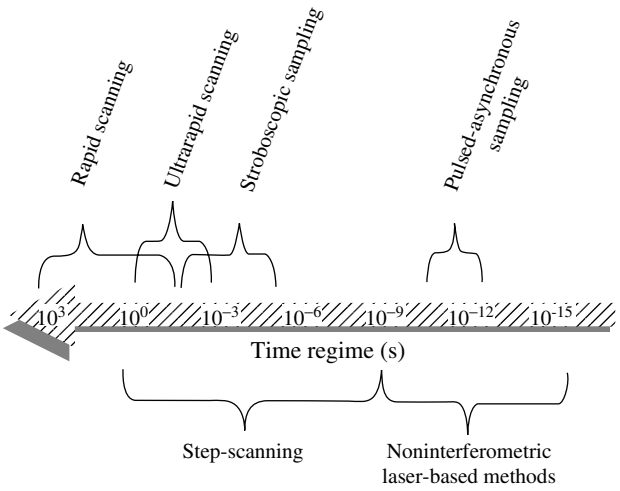

Figure 1. Time scale of FT-TRIR experiments showing applicable range of selected techniques in comparison with laser-based methods.

equipment. For many TRIR experiments, the modest cost and standard availability of time-resolving features on commercial FT-IR spectrometers make their implementation in time-resolved studies throughout the second to nanosecond time scale relatively routine.

This article deals with each of the FT-TRIR techniques indicated in Figure 1. The sections cover the technique's theory of operation, instrumental requirements, specific caveats, advantages and limitations, current applications, and the state of the art. Although every attempt is made to keep the discussion of each technique general, occasionally it is necessary to mention specific instrumentation, and in these cases, the authors have chosen to comment on instrumentation with which they are personally familiar. These instances should not be taken as an indication of the superiority of a particular instrument or piece of equipment, but can be considered at least one proven option for collecting TRIR data. Specific references are intended to direct the reader to more thorough coverage of certain topics in the literature and to applications of each FT-TRIR technique to real chemical problems. Although FT-IR instruments are also used for dynamic measurements in the frequency domain (modulation/demodulation method), these applications will not be covered in this article, and readers are referred to other parts of this work (see Volume 1, Part 2; Volume 2, Part 7; and Volume 4, Parts 1 and 2).

2 RAPID AND ULTRARAPID SCANNING FOURIER TRANSFORM INFRARED

The operation of the classic Michelson interferometer for continuous, or constant-velocity, scanning has been dealt with fully in the literature[6–10] and in this volume (see

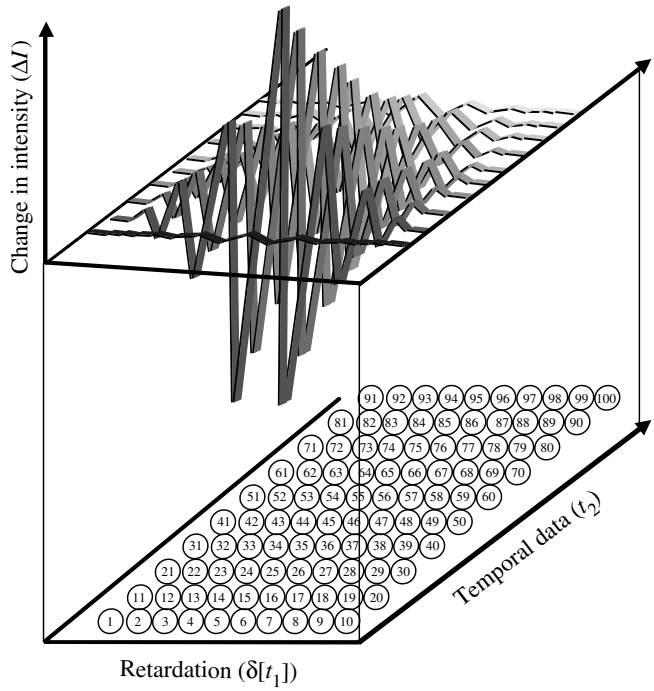

Figure 2. Generation of time-resolved interferograms by use of rapid-scanning FT-IR spectroscopy. Numbered circles below the interferograms show the order of data sampling. When using rapid-scanning FT-IR spectroscopy, data collection proceeds in rows along the retardation axis.

Volume 1, Part 2). In addition to its use for static spectroscopy, it also represents the simplest and most convenient FT-TRIR technique.[11] In rapid-scanning FT-TRIR, the moving mirror's velocity is chosen so that on the time scale of the dynamic event, each scan is effectively instantaneous. Figure 2 shows the data-collection scheme for generating a stack of time-resolved interferograms using rapid-scanning interferometry. For clarity, the interferograms are shown as the change in the intensity (ΔI) during the course of a time-dependent perturbation, and the numbered circles underneath the stack plot display the order in which data are collected by the spectrometer's analog-to-digital converter (ADC). Successive scans of the interferometer collect entire interferograms ($\delta[t_1]$) instantaneously with respect to the temporal evolution of the dynamic event (t_2) so that $t_1 \ll t_2$. The first interferogram (points 1–10) corresponds to the steady state of the sample just before being excited, and in the second interferogram (points 11–20), the state just after excitation.

Typical mirror velocities for standard commercial instruments range from a few hundredths to $\sim 6\,\mathrm{cm\,s^{-1}}$, providing optical velocities of twice those values. The better, more expensive models support a wide range of variability, often extending even beyond these two limits, whereas cheaper instruments offer only a limited number of scan speeds, usually tending toward the middle of the scale where the

mirror is more easily controlled. Thus, for the generation of a $4\,cm^{-1}$ spectrum, the spectrometer requires between 1 s and 40 ms, depending on the scan velocity selected, for the completion of a full pass of the interferometer mirror.

As a general rule, the duration of a scan should be at least an order of magnitude shorter than the half-life of the dynamic event being examined. If this criterion is not met or exceeded, then the intensity of the IR signal will change appreciably over the course of the interferometer scan. The result of such a situation is that transient spectral bands will contribute heavily to the interferogram points collected at the beginning of the scan, but will diminish in intensity by the end of the scan. Such an unsymmetrical waveform will transform into a spectrum laden with noise.

Therefore, assuming that a maximum scan frequency of 25 Hz (40 ms per scan) is available, a dynamic event with a half-life of the order of 500 ms can easily be observed and characterized by multiple time-resolved spectra using rapid-scanning FT-IR spectroscopy and a mercury cadmium telluride (MCT) detector. For much more slowly evolving systems, a lower scan speed and a conventional pyroelectric triglycine sulfate (TGS) detector would suffice. However, with the previously mentioned faster scan rate and high-frequency detector, one could benefit from coadding a number of mirror scans for each time-resolved spectrum in order to increase the signal-to-noise ratio (S/N) while realizing the advantages of the MCT detector's greater sensitivity.

Beyond the aforementioned time scale of several hundred milliseconds, the duty cycle of the conventional rapid (constant-velocity) scanning interferometer is too low to collect an interferogram at a rate significantly faster than the completion of the dynamic event itself. The reason for this limitation is the manner in which the moving mirror is translated along the variable-pathlength arm of the interferometer. This linear motion is often achieved in commercial instruments through the use of a voice coil linear drive motor acting on a mirror that is floating on an air bearing, or air cushion, of some sort.

The impedance to faster scanning of conventional mirrors, say to 1 kHz, originates in the force necessary to quickly move the mirror and reverse its direction after completion of a scan. It has been shown that the force necessary to drive a 30-g mirror using conventional voice coil mirror translation in order to measure a $4\,cm^{-1}$ resolution spectrum in 1 ms (now defined as ultrarapid scanning) is equal to 375 N.[12] This value is well above the typical 1–2 N force generally achieved in commercial instrument voice coils. Although it might be possible to approach the hundreds of newtons required for ultrarapid scanning by some modification of the linear drive motor, the mirror and the bearings required for smooth translation would likely not respond well to such rigorous physical conditions. Furthermore, the inertial force occurring at the point of the mirror's reversal would jolt the spectrometer enough to disturb the other optical components and contribute instability and a large amount of mechanical noise to the measurement.

In spite of the technological difficulties associated with scanning an interferometer at cycles greater than ~25 Hz, the need for an ultrarapid scanning interferometer has spurred new efforts in instrument design to increase the rate of acquiring spectra. Manning and co-workers have identified several areas in which ultrarapid scanning FT-IR spectroscopy would make a significant impact.[13] Three of the areas ripe for the advent of an ultrarapid interferometer are reviewed here.

First, many nonrepeatable and repeatable chemical and physical processes occur on the sub-100 ms time scale and cannot, therefore, be studied using classical rapid-scanning FT-IR spectroscopy. Combustion reactions, impulse spectroelectrochemical experiments, and inelastic polymer deformations are examples of such processes. Remote sensing from rapidly moving platforms, e.g. satellites and airplanes, is another example of a quickly changing observable that is often impossible to repeat, and therefore requires ultrarapid data collection.

Second, in photoacoustic depth profiling, where the thermal diffusion depth varies as the square root of the frequency of modulation of the incident radiation, current modulation frequencies achieved via step-scan FT-IR (see below) or rapid-scanning FT-IR limit the probe depth to values greater than about 1 μm, far too deep for many thin-film studies. A kilohertz scanning interferometer could achieve Fourier frequencies between 100 kHz and 1 MHz. At these modulation frequencies, one would be capable of probing layers as thin as 100 nm, assuming that the available detectors (microphones) are sensitive enough to overcome the inescapable $1/f$ photoacoustic signal reduction that accompanies increasing source modulation frequency.[14]

As a final argument for ultrarapid scanning, the recent surge of progress in FT-IR imaging could receive another boost through the advent of such an interferometer. The state of the art uses a step-scanning FT-IR spectrometer that allows all of the pixels of an MCT focal plane array (FPA) detector to be read out sequentially at each mirror position.[15] This recording scheme can be inefficient since the light delivered to the unsampled array elements is wasted if the readout is slow. With numerous fast ADCs operating in parallel, an improvement not too far on the horizon, one could sample each pixel of the FPA simultaneously while scanning an ultrarapid interferometer at 1000 scans per second. Such an instrument would have the added benefit of maximizing the specific detectivity (D^*) of the MCT detector elements, which increases by approximately one order of magnitude as the modulation of the

incident light is increased from direct current (DC) (as in the step-scan case) to 1 kHz. D^* remains relatively constant from 1 kHz to 1 MHz, which is the typical range of Fourier frequencies for an ultrarapid scanning interferometer operating in the MIR region.[13] Using this detection scheme, an IR camera with over 16 384 units of image resolution (128 × 128 array) and an image capture speed of 1000 frames s^{-1} would be possible. Also, such a camera might possibly outperform current instruments in sensitivity owing to the previously stated advantage of raising the Fourier frequencies of the IR light to the range of maximum detectivity for the detector. From this example and those previously mentioned, the need for an ultrarapid scanning interferometer can be justified.

Various interferometer modifications have been suggested for increasing scanning speeds by switching from translational motion of the mirror to rotational movement. A recent report has outlined the history of these instruments in which an optical path difference is generated via a rotary motion.[12] Many of the initial designs incorporate a tilt-table interferometer in which only a small rotation angle is tolerated by the optical layout, thus leading to a rocking–reciprocating motion. This scheme for encoding the spectral data suffers from the same mechanical limitations as do linear drive motors. More recent designs have utilized a full rotation optical element to generate optical interference. Although this improvement involves a complete revolution, and therefore is capable of being spun with high angular velocity without the negative side effects of a reciprocating movement, the fact that the rotating optical element is the planar salt plate beamsplitter has meant that the maximum scan speeds outside an evacuated bench are limited owing to air resistance. Furthermore, deformations of the rapidly rotating plate are intolerable, and the design still suffers from inefficiency since only a portion of the rotational motion allows for optical interference.

A design introduced by Manning and co-workers in 1999 is shown in Figure 3.[13] This design includes a rotating, highly polished aluminum disk as the rotating optical element. The disk serves as the moving mirror and is cut so that the reflecting surface is angled with respect to the rotation axis, producing a maximum path difference of 0.25 cm over the course of half a revolution. This retardation distance yields a fixed spectral resolution of 4 cm^{-1}. A cube corner retroreflector ensures that the nonplanarity of the incident radiation's wavefront, after leaving the wedge wheel, is tilt compensated by being redirected along the same return pathway. Further rotation of the mirror wheel retraces the 0.25 cm retardation path, thus producing two interferograms per revolution, similar to bidirectional scanning in a reciprocating interferometer. The element can be spun at a maximum of 500 Hz. This mode of operation

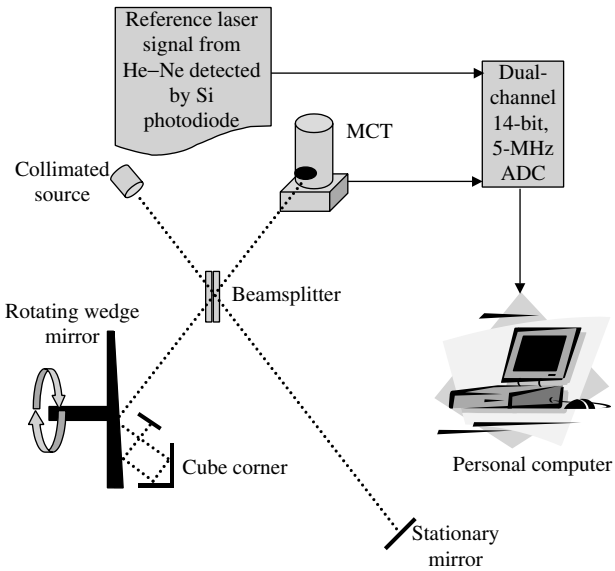

Figure 3. Schematic of an ultrarapid scanning IR spectrometer designed by Manning and co-workers.

will generate 1000 spectra per second, making Manning and co-workers' design the first demonstration of an ultrarapid scanning interferometer as previously defined. The effects of air resistance suggest that vacuum operation will be required for full implementation of this design.

The detection scheme for the ultrarapid scanning instrument described above includes a dual-channel 14-bit 5-MHz ADC to record the two detector signals. The He–Ne laser reference intensity detected using a silicon photodiode and the IR interferogram detected by a photoconductive MCT are digitized simultaneously at the constant sampling frequency of the ADC. Since the zero crossings of the laser interferogram are not used to space (in terms of retardation) the MCT readouts, the laser and IR interferograms must both be interpolated to reconstruct the values of the IR interferogram at the calculated zero crossings of the laser signal. This data processing produces IR interferogram points at equal intervals of optical path difference, a prerequisite for fast Fourier transform (FFT) mathematics, from what are otherwise detector data points at equal temporal spacing.

The ultrarapid scanning interferometer described above has been successfully demonstrated in time resolving the spectral changes associated with the spark combustion of three fuel sources in air: a blackpowder rocket igniter, ethane, and methane. In each instance, the ignition was begun slightly after data collection was initiated, and the dual-channel ADC was then allowed to sample at its normal frequency until the on-board memory was filled. The resulting interferograms were collected at 4 cm^{-1} resolution throughout the entire MIR region at rates of 150–166 scans s^{-1}. At the fastest rate of data collection,

the time-resolved spectra are separated by 6 ms, a factor of seven times faster than that claimed for any conventional rapid-scanning instrument. The spectra reveal both excited emission of the fuel material and the evolution of H_2O and CO_2 from its combustion. The nominal S/N in each instance is ~15 : 1. These demonstrations, however, do not show the maximum time resolution achievable (~1 ms, and perhaps as low as 0.5 ms in the near future), nor the theoretical S/N determined to be possible with this type of instrument.

3 STROBOSCOPIC INTERFEROMETRY

The next faster time regime in FT-TRIR spectroscopy is accessible by the stroboscopic, also called interleaved, FT-IR technique. We do not say it "dominates" this regime because this particular sampling method has only become a standard in a few laboratories where the dynamic events of interest are confined to a time scale from hundreds of milliseconds to several tens of microseconds. In the event that a wider range of time resolution is required, most spectroscopists prefer to invest in the less complicated, albeit more expensive, mode of step-scan operation (see below). However, the inclusion of step-scan FT-TRIR in the spectroscopist's arsenal does not preclude the use of the stroboscopic technique on the same instrument, and in fact many commercial FT-IR research-grade software and hardware packages include an interleaved data collection routine in addition to the step-scan feature as standard components.

Unlike rapid and ultrarapid scanning FT-IR, the stroboscopic method of data collection does not record an entire interferogram in a single pass of the interferometer mirror. Rather, the data collected on a single scan of the moving mirror span a time-resolved set of interferograms that are gradually built up with successive passes of the interferometer mirror.[16,17] The reconstruction of the individual time-separated interferograms requires the use of a clever data sorting routine. Figure 4 shows a schematic view of how the results of an impulse perturbation are time resolved using the stroboscopic method.

The schematic depicts how data collection would be conducted for a flash-initiated reaction that can be reproducibly repeated many times. The cosinusoid represents the interferogram of the He–Ne reference laser as the moving mirror shown below it translates along the interferometer arm. For this explanation, the laser fringes, or zero crossings, are numbered sequentially from 1, the point of zero path difference (ZPD). In the example used here, the mirror's constant velocity is assumed to be such that each laser fringe occurs 10 μs after the previous one, corresponding to a scan speed of 3.16 cm s^{-1} for the translating mirror. The stack plots of interferograms, again shown as ΔI for clarity,

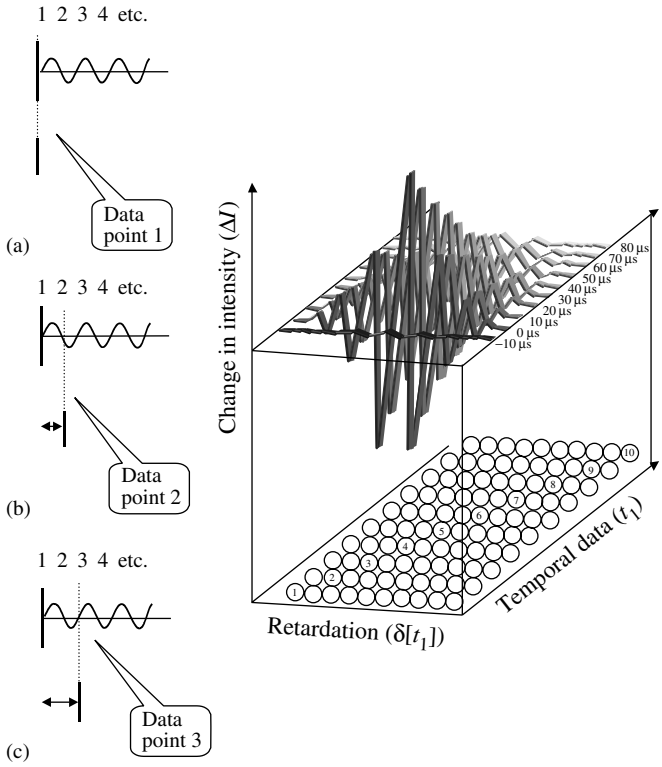

Figure 4. Generation of time-resolved interferograms by use of stroboscopic sampling. The data collection scheme is explained in the text. Numbered circles below the interferograms show the order of data sampling. When using stroboscopic sampling, data collection proceeds diagonally between the retardation and temporal axes.

indicate where data points fall chronologically (shown in the numbered circles) as well as spatially along the retardation axis as they are read off the IR detector. It should be noted that the time scale of the retardation dependence and the time resolution of the measurement are of the same magnitude.

The experiment begins with the interferometer mirror positioned at ZPD (Figure 4a). The detector signal at this point corresponds to a preflash interferogram point that will be used to calculate the background spectrum, shown in the stack plot at $t_1 = -10$ μs. The computer controlling the FT-IR spectrometer is programmed to trigger the short, initiating flash 10 μs into the experiment. This perturbation occurs at the second laser fringe (Figure 4b), and the data point collected here belongs to the interferogram when the dynamic event is first initiated; therefore, the ΔI interferogram has its maximum value. By the third laser fringe, the transient has had 10 μs to decay when the data point is taken (Figure 4c). This data point will contribute to the third interferogram in the time course. The detector sampling continues at a rate of one datum every 10 μs, with each recorded point belonging to the next interferogram in the series.

After the appropriate time decay of the system has been recorded in the first pass, the interferometer mirror is returned to its initial position, and the scan is repeated. However, in order to collect the second point in each of the interferograms along the time-resolved series, the initiation flash is delayed by one laser reference fringe with respect to the previous scan, and data collection begins at the He–Ne fringe just before excitation in order to collect another background data point. In the schematic, this corresponds to data collection at the second fringe and sample perturbation on the third fringe. The "strobed" excitation and sampling continue until enough data have been collected to produce an interferogram for each time delay.

Several caveats of stroboscopic sampling must be further elaborated on at this point. First, the timing of the perturbation event must be strictly controlled. Most commercial FT-IR instruments with this sampling feature provide for a TTL pulse to trigger external equipment responsible for initiating the dynamic event. On subsequent interferometer scans, the software for interleaved scanning incorporates the moving trigger delay.

Second, the reproducibility of the dynamic event is important since the collection of data for the time-resolved spectra requires multiple interferometer scans and multiple repetitions of the time-dependent sample perturbation. This restriction means that the intensity of the excitation source must be nearly identical for every repetition. Similarly, the sample must revert to its original state following the dynamic event without suffering any degradation or attenuation, or alternatively, a new sample must be introduced before the next transient is initiated. Early work using stroboscopic sampling was beleaguered by spectral artifacts that were not discovered as such for some time.[18] Later, other researchers recognized that fluctuations in the number of transients generated per excitation event due to shot-to-shot variations in the excitation source had led to spectral intensity variations that were in-phase with the data collection.[19] The result was a series of artificial "emission" bands that were unfortunately unrecognized as such and subsequently interpreted as originating from the sample's excited state. The discovery of these insidious artifacts has plagued the acceptance of stroboscopic sampling ever since, and the experimental details of any stroboscopic measurement should be considered with caution.

Third, the scanning velocity of the moving mirror must be held at a constant value to guarantee that the temporal acquisition of data is consistent. This latter point is especially important. Triggering the ADC sampling using the He–Ne laser zero crossings removes uncertainties concerning the position of the sampled point along the interferogram, and so it is more reliable than measuring the signal at even intervals of time in rapid-scanning FT-IR of static samples. However, in the stroboscopic sampling method, the exact *position* of the interferogram sampling is also convolved with the exact *time* of the transient sample's decay. Therefore, variations in scanning velocity of the moving mirror will translate into improperly spaced detector readings in time, thus imparting an error into the temporal information recorded at that point in the interferogram. Often this inaccuracy is found to be a random Gaussian distribution of ADC samples around the expected value, thus leading to noise in the transformed spectrum. Many commercial instruments exhibit a 1–2% variation in mirror velocity around the actual value selected in the software.

Weidner and Peale have developed a software package (and modest, optional hardware modification) to be added to commercial instruments in order to decouple the ADC sampling from the temporal He–Ne fringes normally used to trigger data readout.[20,21] Their "event-locked" method samples the interferogram at evenly spaced *times* following the generation of the transient species without concern for the absolute *spacing* of the samples along the interferometer path. The exact, yet uneven, path-length differences of the interferogram data points are determined by continually measuring the precise speed of the mirror throughout its movement. The resulting unevenly sampled interferograms cannot be transformed using the conventional FFT, and so a least-squares fitting routine is necessary. The complete data-handling algorithm and its comparison to standard FFT computations are described completely in the literature.[21,22] The end result is that the event-locked stroboscopic method decreases artifacts and noise associated with mirror velocity variations at the cost of a small increase in expense, data processing time, and computer memory.

Stroboscopic sampling maximizes data collection efficiency not only by multiplexing spectral data via the interferometer, but also by multiplexing the temporal data through the simultaneous collection of multiple temporally resolved interferograms. This feature leads to a tremendous decrease in data collection time versus individually recording an entire interferogram for a single time delay in a pseudo-pulse/probe manner. For instance, in a typical interferometer scan, over 1000 data points must be taken to achieve reasonable spectral resolution over the entire MIR region. To collect a single time-resolved spectrum, the reaction of interest would need to be repeated 1000 times with the appropriate excitation delay synchronized to the ADC sampling at each He–Ne fringe. To collect a time-resolved group of 20 spectra, a total of 20 000 flash-initiated events would have to be reproduced exactly. This requirement places an unacceptably large obligation on the instrument, excitation, and sample stability.

The duty cycle of the stroboscopic method can be further increased if the event of interest is relatively short lived in

relation to the time required for a single scan. For instance, if we assume that the spectral range and resolution in the example used for Figure 3 require a 1000-point interferogram (therefore taking 10 000 μs to complete), and that the sample's dynamic changes are fully completed in 200 μs, then we can potentially repeat the experiment 50 times over the course of one sweep of the interferometer mirror. In effect, 50 data points will be added to each time-resolved spectrum with each pass of the mirror. Hence, a total of only 20 mirror scans and 1000 laser shots will be necessary to generate 20 time-resolved spectra of the dynamic event, an increase of over 20-fold in data collection efficiency compared with the individual spectrum method described above.

Stroboscopic sampling is a relatively inexpensive means of performing TRIR on transient samples with a maximum time resolution of ~1 μs. The only instrumentation required is a standard FT-IR spectrometer capable of synchronizing an external excitation source. The rest of the technique's parameters are software controlled. The upper limit in time resolution is enforced by the maximum mirror velocity that the spectrometer can achieve, and there is a large degree of variability in mirror velocities between different makes and models of spectrometers. Many top-of-the-line commercial instruments provide a wide range of mirror velocities ranging from about 0.03 to 6 cm s^{-1}. Less expensive models may only allow a limited number of choices, and normally these options are restricted to the intermediate range of the velocity spectrum.

A final, yet limited, application of stroboscopic sampling serves as a good segue to the description of one of the fastest growing interferometer-based TRIR techniques, step-scan FT-IR time-resolved spectroscopy. In the event that the transient of interest has a lifetime that is very short with respect to the delay between He–Ne laser fringes, a limiting case of stroboscopic sampling exists.[1] In this distinctive case, the transient can be generated by a quick perturbation at each He–Ne fringe. Following the perturbation, a fast gated detector is used to sample the transient IR signal at equal time intervals throughout the decay of the dynamic event. Figure 5 shows the data collection scheme for this stroboscopic variant.

Although the mirror continues to move during the detector's successive readouts, the relatively small position deviations along the time series of measurements are inconsequential if the phase shift introduced is small with respect to the spacing of He–Ne fringes (<1%). If the phase shift is larger, then it can be removed by software prior to Fourier analysis. This positional error can be minimized by decreasing the mirror velocity so that the sampling rate is several orders of magnitude faster than the Fourier frequency of the He–Ne laser.

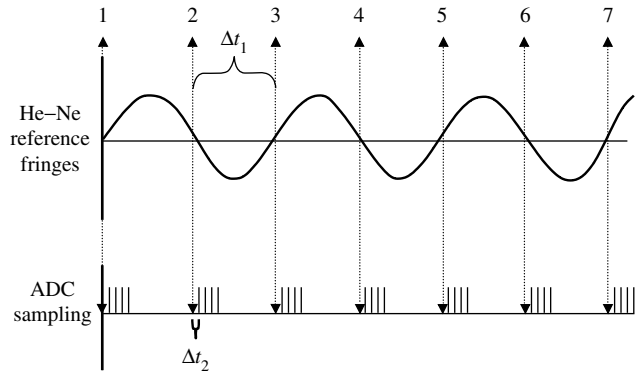

Figure 5. The limiting case of stroboscopic sampling requires the rapid triggering of equally spaced ADC samples following each zero crossing of the He–Ne reference laser. Δt_2 must be much smaller than Δt_1. Other stringent restrictions apply to this form of FT-TRIR and are discussed in the text.

At the end of the scan, a number of interferograms equal to the number of ADC samples taken at each laser zero crossing will have been generated. The time delay between subsequent interferograms can be as short as ~10 ns using a fast photovoltaic (PV) MCT detector and a 100-MHz transient digitizer. Moreover, because the accuracy of the time resolution is solely a function of the degree of control between the excitation pulse and detector gate, i.e. it is decoupled from the scanning velocity of the interferometer mirror, this technique of FT-TRIR is less prone to temporal artifacts than the typical stroboscopic method.

It is important to note that serious restrictions apply to this simplified stroboscopic method. First, the *minimum* rate of digitization is limited by the slowest mirror velocity available, usually relegating the transient sampling to less than 5 μs per time slice. This requirement exists because a complete set of temporal data points must be collected before the mirror has translated a significant portion of the distance toward the next He–Ne laser fringe. If the temporal recording of data extends to greater than a few percent of the time delay between He–Ne fringes, then the sampling position inaccuracies for each time-resolved interferogram become so great as to introduce a substantial amount of noise into the transformed spectra.

A second, but related, restriction is that the transient species that are appropriate for this time-resolved technique must have lifetimes shorter than ~100 μs. If the lifetime of the transient is appreciably greater than this value, a significant population of molecules will still be in the excited state by the onset of the next perturbation event, even at the modest interferometer scanning rate previously mentioned. If this situation were to occur, then the experiment would violate the paramount requirement of stroboscopic sampling, namely reproducible generation of the transient species.

Third, the need to repeat the excitation at every reference laser fringe requires sample excitation at a minimum rate

of 1 kHz, provided that a suitably slow mirror scan velocity is available. This repetition rate is a fairly stringent demand, for example, when the experiment necessitates high-powered laser excitation. Even with significant undersampling of the interferogram, this requirement can be a challenge. Overall, the limiting case of time-resolved stroboscopic FT-IR spectroscopy has particularly restrictive provisions, and there exist few applications that can meet them all.

Stroboscopic sampling has developed a devoted, yet modest following among IR spectroscopists. Much of the recent work using this technique has been generated by Leone and co-workers using IR emission and the classic stroboscopic method[23–26] and by Sloan and co-workers using IR absorption and the limiting case of stroboscopic sampling.[27–29] Their numerous investigations into gas-phase kinetics, including reaction dynamics, intermediates, and energy transfer rates, give an interesting and up-to-date account of the applications and potential of the stroboscopic technique. However, for the study of many shorter-lived as well as longer-lived transients, a more recently commercialized FT-TRIR technique, step-scan FT-IR time-resolved spectroscopy, has become vital and widely applied.

4 STEP-SCAN INTERFEROMETRY

Although the ultrarapid scanning and stroboscopic methods extend the capabilities of continuous-scan FT-IR to include relatively fast dynamic measurements, routine continuous-scan FT-IR is ultimately limited to analyzing processes whose duration extends a few hundred microseconds, at least as long as a continuous-wave (CW) source such as a globar is used. This limitation is imposed because the time dependence of the dynamic measurement is interwoven with the time response of the sample. In essence, the recording of the interferogram using a CW source and a constant-velocity FT-IR instrument is itself always a function of time. This complication has given rise to a renewed interest in step-scanning interferometry since the 1980s and its application to time-domain spectroscopy, particularly on the submicrosecond time scale where few other techniques can compete (see Figure 1).

The step-scan method, originally developed in its modern form in the early 1960s, saw only limited application until the early 1990s.[4,30–33] The novelty of the technique lies in its ability to decouple the time dependence of the IR measurement from the time dependence of the dynamic event being investigated. In effect, it is analogous to the limiting case of the stroboscopic method described above except that the mirror velocity is now infinitely slow. In step-scanning interferometry, the mirror retardation is achieved in discrete jumps, or steps. At each retardation point, the "moving" mirror is held still while data are collected. Time-resolved data at each position in the interferogram can be recorded following an excitation event, and multiple data points at that constant retardation can be successively coadded if necessary to achieve a higher S/N. At each discrete point in the interferogram, the spectral multiplexing is effectively decoupled from the time domain, i.e. there are no temporal Fourier frequencies, so any degree of time resolution with any S/N and any spectral resolution is theoretically possible.

Figure 6 shows the data-recording scheme used in the step-scan mode of FT-TRIR. The data are collected in time-resolved columns (temporal data) at each point along the row of interferogram retardation points (δ, interferogram data). At each position in the interferogram row, the transient is created and the IR detector is sampled at a set time interval along the temporal axis until the sample has fully relaxed. The first sequence of recorded data is shown by the numbered circles in the first column (points 1–10). At this point, the sample excitation can be identically repeated and the data averaged along the same temporal column to improve the S/N (again, 1–10), or, if an appropriate S/N has already been achieved, the mirror can be moved to the next point in the interferogram and the excitation repeated to collect the second column of temporally resolved data (points 11–20).

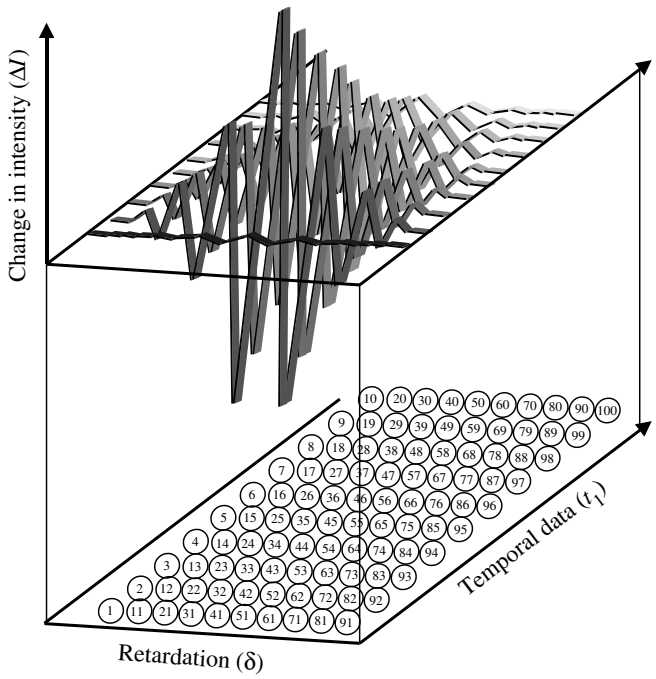

Figure 6. Generation of time-resolved interferograms by use of step-scanning FT-IR spectroscopy. Numbered circles below the interferograms show the order of data sampling. When using step-scanning FT-IR spectroscopy, data collection proceeds in columns along the temporal axis.

This cycle is repeated until each interferogram data point has been collected for the required spectral range and resolution of the experiment. The three-dimensional array of data is then sorted into time-resolved interferograms and subjected to FFT to generate a stacked plot of time-resolved spectra. In order to improve the S/N, the results of two or more sequential step-scan data sets can be coadded. The dynamic event, like that in stroboscopic sampling, must be infinitely repeatable and exactly reproducible over the length of the experiment or else the S/N will be severely degraded. This requirement extends to the integrity of the sample over time as well as to the intensity of the excitation event with each cycle.

Several experimental safeguards have been used to guarantee that the these requirements are met. When studying irreversible reactions, flow cells for liquid or gas reagents[34,35] and rotating or translating sample stages for other samples[36] have been used to assure fresh sample is introduced into the path of the IR radiation with each cycle of the dynamic event. This strategy is also useful when monitoring the early stages in a dynamic event with an inconveniently long lifetime.[37] It is also important that the population of excited molecules is nearly identical with each cycle of the dynamic event. As an example, high-power laser sources, which often vary in shot-to-shot intensity by as much as 10%, present a challenge for generating comparable numbers of excited-state molecules with each pulse. In order to ensure reproducible excitation, the results of numerous laser shots can be coadded at each interferogram position to achieve a reproducible average value, or the laser intensity with each shot can be detected with a photodiode and made to fall within a specified range before accepting the temporal data for that interferogram position. Alternatively, the excitation intensity can be monitored and used to normalize the spectral response to each laser pulse. Clearly, the requisite reproducibility and repeatability for step-scan data collection can be met for nearly any dynamic event if suitable precautions are taken.

Dynamic step-scan FT-IR spectroscopy offers several advantages over continuous-scan techniques (ultrarapid scanning and stroboscopic sampling) as well as IR laser, dispersive, frequency mixing, and upconversion methods of TRIR. In contrast to continuous-scan instruments, the step-scan mode of data collection is only restricted in terms of time resolution by the speed and sensitivity of available IR detectors, amplifiers, and digitizers, as well as the temporal profile of the excitation source. Since the mirror is held constant during data collection, there is no *fundamental* limitation imposed by the technique to the speed, whether slow or fast, at which temporal data can be recorded. Furthermore, the step-scan mode of data collection offers a simpler alternative to the complicated and calculation-intensive stroboscopic method without the concern for spectral artifacts arising from mirror velocity uncertainties.

Step-scan FT-TRIR, however, is currently limited to time resolution of the order of ~1 ns owing to the state-of-the-art detector and electronics technology available, and therefore falls below the temporal resolution achievable with tunable laser and laser-mixing techniques. Despite this shortcoming, the use of the step-scan mode for nanosecond-regime applications excels in terms of the spectral range and resolution that can be realized with relatively short data collection times. The limited range and tedious tuning of the laser sources used in many ultrafast TRIR techniques make the collection of high-resolution, broadband spectra particularly frustrating. As a result, applications of step-scan FT-IR for time-resolved spectroscopy have surged (see below).

The instrumentation necessary for step-scan FT-TRIR is less costly than that required for the ultrafast laser methods, but more expensive than that demanded for stroboscopic sampling. The addition of the step-scan mode of interferometer movement adds considerably to the expense of the FT-IR instrument and generally pushes the user into the realm of research-grade spectrometers. Furthermore, three areas of instrumentation and electronics must be considered in adapting step-scan interferometry to time-resolved studies. First, a means to synchronize the sample excitation, data collection, and interferometer stepping must be considered. Second, the appropriate detector and digitizer must be selected for the time regime and budget of the experiment. Finally, in some step-scan interferometers, e.g. the BioRad FTS 60A/896, the stepping mirror's "dither", the rapid modulation used in positioning the mirror, must be demodulated from the transient signal of interest.[38,39]

Synchronization of the experiment's excitation source, data collection, and interferometer movements can be arranged in two ways. The most convenient manner of timing is to use an external digital pulse generator to serve as the master experimental clock. This arrangement benefits from the timing accuracy of the pulse generator, its low phase jitter (normally <0.5 ns), and its ability to manage complex triggering patterns. In a typical experiment, the pulse generator will send a trigger signal to the FT-IR bench or transient digitizer to mark the beginning of data collection. The digitizer will then initiate a stream of detector samples, evenly spaced according to the preset time resolution of sampling. A second trigger signal from the master clock will then be sent to the excitation source after a preprogrammed delay. This trigger will initiate the sample perturbation (via laser pulse, rheometer motion, electric field pulse, reagent mixing, ignition, etc.).

Software controlling the digitization will allow data recording to proceed to a preset interval along the decay of the sample. If the software is programmed to coadd

numerous laser pulses at each step in the interferometer, then the mirror will remain fixed while awaiting the next excitation cycle. The next transient event will occur after a sufficiently long delay to allow the sample to recover fully, or in the event of an irreversible process, for new reagents or sample to enter the path of the IR beam. Then, the pulse generator triggering cycle is repeated as above. If, however, the number of coadditions has been met, the FT-IR bench steps the mirror to the next position along the retardation path and prepares for the next triggering sequence. It is normally imperative that the short triggering pulses be transmitted via 50-Ω cabling/BNC connector combinations since the digitizer circuits are sensitive to impedance mismatches that could lead to signal attenuation or ringing along the coaxial cable.

The second option for experiment synchronization is to use the FT-IR bench's software for sequence timing. Most commercial software and bench electronics allow for internal experiment triggering and preset data collection delays. It is possible to use these features to synchronize the sample excitation, transient detection, and mirror stepping. For instance, the spectrometer can be set to step at a predetermined rate, say 10 Hz. At each mirror step, the software triggers the external sample excitation source following a preset delay to allow for mirror stabilization and the initiation of data collection before the perturbation. Using the stepping frequency of the interferometer mirror as the master clock precludes the coaddition of data at each position in the interferogram. However, multiple passes of the interferometer can be signal averaged to increase the S/N of the resulting spectra. This scheme for signal averaging can, in the end, be beneficial since it removes the influence of slow drift of electronic and optical components. Its major drawback is that the stepping cannot be much faster than 10 Hz and still allow the tens of milliseconds necessary for mirror stabilization, and so the repetition of the transient event is also limited to this low duty cycle.

The second consideration for adapting step-scan FT-IR to time-resolved measurements is the proper selection of detectors, amplifiers, and digitizers. Again, the modes of recording data are generally divided into two categories that can be identified by the detector coupling that is used, namely DC or alternating current (AC) detection. The DC method, the least expensive and less complicated means of collecting the data, utilizes the internal ADC of the FT-IR bench as the data digitizer. Most on-board ADCs operate at a maximum rate of 200 kHz with ~16-bit amplitude resolution, thus limiting time resolution to a maximum of 5 μs between temporal data points. If this is acceptable, a common photoconductive MCT and amplifier (typically 1 MHz, ~250 ns rise time) can be used to sample the transient IR signal.

Unlike most IR detectors, the photoconductive MCT in this instance is DC-coupled to prevent any low-frequency filtering. This configuration can be contrasted with the typical AC-coupled detector where an RC circuit is used to remove frequencies below 10 Hz. AC coupling is normally preferred as a convenient means of eliminating slow changes in instrument operation and thus limiting spectral noise in a conventional rapid-scan measurement while maximizing the digitization resolution of the ADC. However, when measuring the decay of transient species with lifetimes of the order of several milliseconds, the lower filtering limit must be overridden via DC coupling to prevent losing portions of the transient signal. Following detection of the dynamic signal, the acquisition processor (AQP) stores the data in on-board memory until the end of the experiment, after which they are subjected to FFT and saved to hard-disk memory.

To take advantage of the highest time resolution capable in step-scan operation, a specialized transient digitizer must be used, in addition to a high-bandwidth PV MCT. Most of the major FT-IR instrument manufacturers that offer a step-scan feature can supply at least a 100- or 200-MHz transient recorder that is programmed to work with their instrument software to collect fast time-resolved spectra. However, because of the operation speed of the transient recorder, these boards often come with only 8–12-bit digitization. An example of this type of data recorder is the Spectrum PAD82a. The PAD82a is housed on the motherboard of the personal computer responsible for controlling the FT-IR bench. It accepts a trigger input, two channels of data, and an external sampling trigger. The board typically operates at 100 MHz when simultaneously using both channels to record two signals, but it can digitize at 200 MHz if only one signal is being recorded.

To realize the sampling rate of the transient digitizer and maximize its sensitivity, an AC/DC dual-output PV MCT with a fast preamplifier is required. The speed of the detector must be at least as great as the digitization rate of the transient recorded, otherwise the time-resolved data will be convolved with the rise time of the detector. With a dual-channel detector, the AC output is used to carry the transient changes in the interferogram at the position being monitored. The switch from a DC signal, as in the previous case, to an AC signal is employed in order to maximize the smaller dynamic range of the 100-MHz digitizers. However, a 50-MHz preamplifier has been described that combines the optimum utilization of dynamic range offered by AC coupling with the broadband sensitivity of DC coupling. The quasi-DC-coupled preamplifier removes the lower frequency limit of standard AC-coupled detectors (~1 kHz) so that dynamic events with interesting kinetics over a wide time scale (nanoseconds to milliseconds) can

be monitored in a single experiment with maximum digitization sensitivity.[40]

It is important to note, however, that the collection of an AC interferogram introduces a new complication to the postcollection data manipulation. Being an AC signal, these data can contain both positive and negative intensities. The final Mertz or Forman phase correction routines of the FFT are unable to handle interferogram data that contain negative signed components. Therefore, a DC signal is collected separately, but simultaneously, at each mirror position and the resulting DC interferogram is later used to phase correct the AC interferograms. Although a stored phase from a previous DC spectrum could be collected ahead of time and used later for phase correction of the AC time-resolved interferograms, the concurrent collection of a DC interferogram with the AC interferograms eliminates any phase inaccuracies that might occur between the two experiments. Kolmar Technologies provides a dual-channel PV MCT and fast preamplifier (100 MHz, Model KV104) with an 11-μs cutoff and theoretical rise time of 3.5 ns. With the increasing miniaturization of electronics, one can expect to see even faster detectors in the near future that benefit from the summing of multiple independent MCT elements, each using its own preamplifier. However, for the time being, using the maximum sampling rate of the transient digitizer described above, and recording both the AC and DC channels of the KV104, this detection and recording arrangement can achieve a maximum time resolution of ~10 ns.

Figure 7 shows the experimental setup employed by the present authors for collecting nanosecond regime flash photolysis time-resolved spectra with a step-scan FT-IR spectrometer, digital pulse generator, AC/DC dual channel PV MCT, and transient digitizer.[5] The time-resolved measurement begins with the stepping mirror in the ZPD position. The pulse generator initiates the experiment by triggering the laser flashlamps to commence population inversion within the laser cavity; a Pockels cell, or Q-switch, prevents lasing at this point. After an appropriate delay, the pulse generator sends a second trigger to the transient digitizer to activate data collection. The AC signal from the PV MCT is recorded at a constant time interval preselected using the computer software. A single DC data point is also recorded from the second, DC-coupled detector preamplifier. A third trigger activates the sample excitation source, and the laser pulse generates the transient species instantaneously on the time scale of the experiment. Throughout this process, data digitization of the AC signal continues at the software-selected rate, thus yielding temporal data both before and after the sample's excitation.

The software recognizes if multiple coadditions were requested, and allows multiple triggering events to occur at the current mirror position. The PAD82a transient digitizer averages these repetitions on the fly, and following the last excitation cycle, the temporal data are transferred to the AQP where they are stored in on-board memory. The PAD82a, unlike some other digitizers, has a zero latency period for data transfer, and so the shuffling of data during the course of the measurement does not diminish the normal duty cycle of the experiment. After the AQP has received the data, the mirror is stepped to the next mirror position, and the PAD82a board is signaled to begin collecting the next DC data point and temporal AC data column following

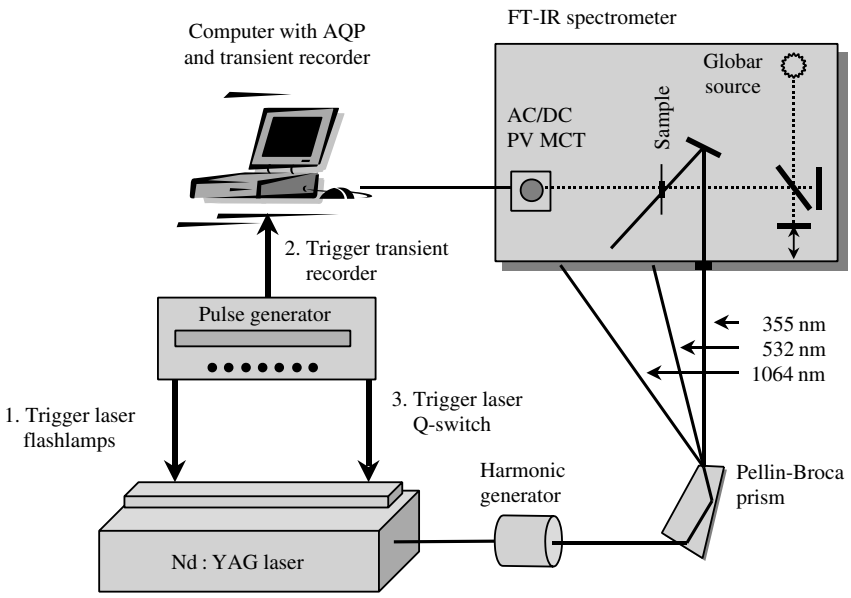

Figure 7. Experimental setup for collecting nanosecond regime, broadband MIR time-resolved spectra of a laser-induced transient species using a step-scan FT-IR spectrometer.

the subsequent trigger pulse from the signal generator. This process continues until all the data have been recorded, or until the on-board memory of the AQP has been filled.

Once the full data set has been recorded and passed to the AQP, each of the AC interferograms is sequentially phase corrected using the DC interferogram and subjected to FFT to generate a time-resolved array of intensity difference (ΔI) vs wavenumber spectra. These data can then be processed into an array of absorption difference (ΔA) spectra for subsequent interpretation.

Several variations for recording nanosecond FT-TRIR data have been demonstrated, some of which seek to reduce costs whereas others attempt to increase the time resolution of the step-scan technique. The added expense of a dual-channel PV MCT, required for collecting the DC interferogram for successful phase correction, can be circumvented by using a clever double-angle phase-correction algorithm described by Hutson and Braiman.[41] Their correction routine overcomes the obstacle of positive and negative signed intensities in the AC interferograms by convolving a double-sided transient AC interferogram with itself. The convolution doubles the phase angles, thereby removing phase-angle discontinuities present in the data due to sign changes. The double-angle phase correction technique represents a significant advance over the Mertz Signed phase-correction routine and reduces the cost of the PV MCT by allowing a single-output detector to be used. However, this direct phase-correction technique requires complete, double-sided interferograms to be measured, and therefore the time spent collecting data using this method is twice that expended with a two-channel detector capable of simultaneously measuring a DC-coupled interferogram.

For faster time resolution, Johnson and co-workers reported a variation on the step-scan transient data collection routine using an 8-bit, 2 Gsample s^{-1} digital storage oscilloscope (DSO) acting as the transient digitizer rather than a PC-based digitizer like the PAD82a.[3] The DSO works in conjunction with the standard instrument-control software and an additional, commercially available, data-transfer module, the McLaren Research TM1000, and its associated software. This upgrade can be implemented fairly easily since many laboratories already possess a fast DSO for laser and electronic diagnostics, leaving only the data transfer module to be purchased for ~$10 000. The time-resolved signals are recorded by the DSO digitizer, transferred to PC memory, reconstructed as a slower waveform via a 20-μs digital-to-analog converter (DAC), and then fed back through the FT-IR instrument's ADC at its normal digitization rate, usually around 200 kHz.

The DSO-sampled data that are demonstrated in the original report are from the visible emission of a dye laser-pumped NO_2 gas cell. The ~2.5-ns time resolution of the experiment was limited by the rise time of the photomultiplier detector. However, with the high sampling rate of the DSO, the resolution could theoretically be as high as 500 ps. This value can ostensibly be decreased as newer DSO and detector technology is introduced. As yet, subnanosecond data collected in the MIR region have not been reported in the literature, although a Bruker Optics product note reports true 10-ns time resolution for the output of a pulsing MIR (~6450 cm^{-1}) diode.

As previously mentioned, the advantages of the DSO-based method include the higher time resolution of the oscilloscope data collection versus currently available PC-based digitizers and the ability to use hardware already available in many laboratories. Moreover, several other benefits can be realized. First, the DSO method demonstrates a fivefold increase over ISA-bus transient digitizer boards in the S/N of resulting spectra. This increase has been attributed to the isolation of the oscilloscope digitizer from the PC electronics, and also the increased accuracy of the DSO trigger response. Furthermore, the ability to store raw data on the PC's hard disk before sending it through the final software algorithms allows the results of various apodization, zero-filling, and phase-correction manipulations to be examined without the loss of the original data. The data can also be scrutinized to be certain that they meet certain boundary conditions, such as an excitation laser intensity threshold as measured by a fast photodiode. However, experiment-based specifications such as frequency range, spectral and phase resolution, and double- or single-sided nature of the interferogram are not alterable.

One drawback of the DSO technique is that the duty cycle of the data collection is limited by the data-transfer rate of the DSO to the transfer module, TM1000. The data recorded at each mirror position in the interferometer must be moved ultimately to computer storage before the transient signal at the next position is recorded. This latency period is larger than that of PC-based digitizer boards. The current transfer limit stands at about 30 Hz, which is actually well beyond the repetition rates of many of the currently popular high-energy laser excitation experiments that operate at ~10–20 Hz. However, since the limit is not intrinsic to the equipment, but rather to firmware and software, one can expect the data-transfer rates to improve with new technology.

The final consideration for using conventional step-scan instruments for fast time-resolved spectroscopy involves only those instruments that use a phase jitter on the stepping mirror for position control.[38,39] The phase dither, although allowing for constant dynamic alignment of the mirror's position, adds an unfortunate complication to the measurement of time-resolved spectra. The constant phase modulation of the mirror generates its own transient signal,

and this signal's amplitude is normally far larger than that of the transient event being measured. Therefore, techniques must be used to demodulate the mirror's movement from the signal of interest.

The most successful procedure for eliminating the instrument's transient signal has been to synchronize closely the phase of data collection and sample excitation with the phase of the mirror dither.[42] In BioRad's FTS 60A/896, the mirror dither is a constant 16 kHz. By detecting with a gated boxcar integrator set 62.5 μs before the sample is excited and a second integrator coincident with the sample's excitation, the effect of the mirror's dither can be removed. The instrument-derived signal is nulled because the matched gates are exactly in-phase with the mirror's dither, and therefore, when the "light off" (62.5 μs before excitation) and "light on" signals are ratioed such that $\Delta A = -\log(\text{light/dark})$, the absorption difference spectrum no longer contains the transient from the mirror modulation. This calculation, however, only yields a single excited sample spectrum rather than a time-resolved group of spectra. Although further modifications can be used to generate the required data set, they are not without added difficulty and cost. Clearly, for the fast time-domain experiment, the benefits of the positional accuracy allowed by the mirror modulation are arguably dispensable.

The time regime in which step-scan FT-IR dominates is particularly rich in applications. The literature is laden with examples of step-scan FT-IR being used to collect broadband MIR spectra of dynamic systems. A few examples include studies of biological photocycles,[43,44] organic reactions in zeolites,[45] small ligand binding to biological proteins,[46] impulse photoacoustic measurements,[47] mechanisms of pericyclic ring openings,[35] hydrosylation bond activation,[34] time-domain polymer rheology,[48,49] protein folding dynamics,[50] and inorganic complex excited states.[51–54] As step-scan FT-IR becomes more widely known in the scientific community, and as the time resolution of the technique creeps closer to the picosecond regime, further applications and more widespread use are a certainty.

5 ASYNCHRONOUS SAMPLING

The final technique in FT-TRIR spectroscopy, asynchronous sampling, has been dealt with previously in terms of instrumentation. Therefore, the instrumentation and theory will be dealt with in only a cursory fashion here. First, it should be emphasized that the asynchronous technique is applied with a standard rapid-scan interferometer. Step-scanning is not involved. With asynchronous sampling, two possibilities exist: a CW probe mode (globar) or a pulsed probe mode. In either case, the repetition rate for creating the transient event must conform to the Nyquist requirement, i.e. it must be $\geq 2 \times$ the highest Fourier frequency in the spectral range. A repetition rate of 10-fold greater than the highest Fourier frequency is often used for good measure.

The essence of the asynchronous sampling technique is that the sample perturbation is not timed with respect to the scanning and data acquisition of the spectrometer, i.e. the two are *asynchronous*. It is also worth noting that the standard asynchronous sampling technique gives a single time-delayed spectrum with each experiment. However, for the CW mode, a multichannel gated device is available from Sopac Corporation and S. T. Japan, Inc. that allows the collection of up to 16 time-resolved spectra in one experiment.

In either the CW or pulsed mode, the fundamentals of the signal processing are identical for the collection of a single time-delayed spectrum. The signal generation and processing for a single IR wavelength is shown in Figure 8. This simple example is illustrated for the purpose of explaining the principles of the technique, but in an actual asynchronous sampling experiment, the signal, data collection, and processing involve the entire interferogram and are thus the sum of all frequencies of the IR source. The constant-velocity interferometer modulates each frequency of the source at its characteristic Fourier frequency (Figure 8a). The sample perturbation induces spikes in the sinusoidally modulated intensities corresponding to each wavelength in the spectrum, at intervals of τ, where τ is the spacing between perturbation events (Figure 8b). Sampling the decay of these spikes at a delay of $\Delta\tau$ following the perturbation (Figure 8c) using a gated detector (or a probe pulse) produces a "discrete" high-frequency interferogram "carried" by the normal analog interferogram (Figure 8d). Low-pass filtering of the signal recovers the analog interferogram, but now with the intensity of each of its frequencies altered to reflect the spectral band intensities at time $\Delta\tau$ (Figure 8e). This interferogram is then sampled at the ADC's normal digitization rate, which according to the Nyquist theorem should be at least twice the highest Fourier frequency.

As mentioned, signal recording in the CW mode is performed with a narrow gate applied to the detector at $\Delta\tau$. In the pulsed probe mode, the gate is replaced by a probe pulse delayed with respect to the pump pulse by $\Delta\tau$. The gate width is similarly replaced by the width of the probe pulse. In both instances, the limit to the time resolution comes from the pulse width of the excitation source, the temporal accuracy of $\Delta\tau$, the narrowness of the gate or probe pulse, and (in the CW mode) the rise time of the detector. The final data collection results from the ADC sampling of the analog interferogram after low-pass filtering.

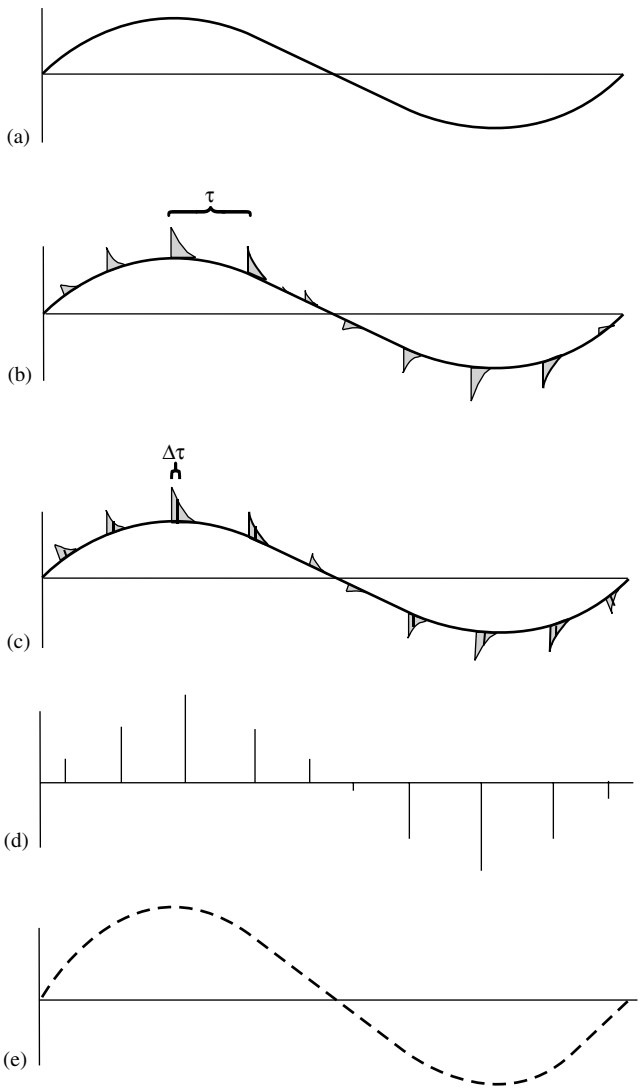

Figure 8. Data collection scheme for asynchronous sampling. For simplicity, only the Fourier modulation of one wavelength of light is shown (a). This wavelength is further modulated by perturbation pulses at intervals of τ (b). Each perturbation is followed by a probe at $\Delta\tau$ after the perturbation (c). The detector gate or probe pulses generate a discrete interferogram (d) that is converted back to an analog interferogram for time $\Delta\tau$ by the low-pass filter where the interferogram is sampled by the spectrometer's ADC at its normal rate (e).

The CW asynchronous sampling method, first proposed and demonstrated by Masutani *et al.* in 1992,[55] has been described in detail elsewhere in this volume. It has been shown to be particularly valuable in the study of the microsecond reorientation dynamics of ferroelectric liquid crystals in response to pulsed electric fields.[56,57] Although nanosecond range time resolution is possible, the same detector rise time limitation applies here as in the step-scan method, which also uses a CW source. It is also worth noting that the requirement of relatively high repetition rates, to move the perturbation frequency well outside the Fourier frequencies, means that only relatively rapid processes can be studied since the sample must fully relax before the next perturbation event. For example, a 10-kHz perturbation rate can easily be a 10-fold increase over the highest Fourier frequency in the MIR range at moderately slow scan speeds, but such a repetition rate requires that the sample's excited-state half-life be less than $\sim$30 μs. Also, certain low repetition rate lasers (e.g. a high-power Q-switched Nd : YAG laser) are unsuitable as excitation sources. Thus the CW mode of asynchronous sampling overlaps the faster time regime of step-scanning FT-IR spectroscopy (100 μs to 1 ns), but, unlike step scanning, it cannot be applied to longer time scales.

The pulsed probe asynchronous sampling technique, on the other hand, has the potential to open up the sub-nanosecond and possibly subpicosecond time regimes to interferometric techniques. The possibility of the pulsed probe experiment was first suggested by Masutani *et al.* in their original publication,[55] but since then it has been demonstrated only in time-resolved resonance FT-Raman (FT-TR^3)[58,59] and in a closely related experiment in the far-IR region using a pulsed synchrotron source.[60] The important factor here is that the time resolution in such a pulsed pump–probe technique depends only on the widths of the pump and probe pulses and the accuracy of their relative timing, not on the rise time of the detector.

In the pulsed asynchronous sampling mode, the fast repetition rate of the pump (and now probe) pulse is still required. Its application in the MIR region requires a high repetition rate pulsed source that is broadband and temporally narrow, features not found in most conventional IR sources. As pointed out by the originators of the technique, the most promising source is probably synchrotron radiation,[61] and a number of research groups are working to demonstrate such an experiment in the MIR region at synchrotron storage rings around the world.[5,60,62] The pulsed output of a synchrotron is normally in the range of megahertz, and this feature may restrict its application to even shorter-lived transients than previously mentioned unless appropriate steps are taken to reject a portion of the pulses from being recorded by the detector. As more progress is made in developing this method of FT-TRIR, one can expect interferometric techniques to begin to challenge laser-based methods in the ultrafast time regime.

6 SUMMARY

In this article, we have systematically reviewed the ways in which FT-IR spectroscopy, with all its associated advantages, has been used in the measurements of time-dependent phenomena and transient species in the MIR region. These methods span time-resolution capability from >1 s to <1 ns

and are capable of measuring transient absorptions as small as 10^{-4} absorbance units. The upper time resolution limit will continue to decrease for FT-TRIR techniques as new detectors, digitizers, and broadband IR sources become available.

ABBREVIATIONS AND ACRONYMS

AC	Alternating Current
ADC	Analog-to-digital Converter
AQP	Acquisition Processor
CW	Continuous-wave
DAC	Digital-to-analog Converter
DC	Direct Current
DSO	Digital Storage Oscilloscope
FFT	Fast Fourier Transform
FPA	Focal Plane Array
FT-TR^3	Time-resolved Resonance Fourier Transform-Raman
FT-TRIR	Fourier Transform Interferometric Time-resolved Infrared
TRIR	Time-resolved Infrared
TRS	Time-resolved Spectroscopy

REFERENCES

1. J.J. Sloan and E.J. Kruus, in "Time Resolved Spectroscopy", eds R.J.H. Clark and R.E. Hester, John Wiley & Sons, Chichester, 219, Vol. 18 (1989).
2. A. Laubereau and M. Stockburger (eds), 'Time-resolved Vibrational Spectroscopy', Springer, Berlin, Vol. 4 (1985).
3. L.T. Letendre, H.-L. Dai, I.A. McLaren and T.J. Johnson, *Rev. Sci. Instrum.*, **70**, 18 (1999).
4. T.J. Johnson, A. Simon, J.M. Weil and G.W. Harris, *Appl. Spectrosc.*, **47**, 1376 (1993).
5. R.A. Palmer, G.D. Smith and P. Chen, *Vib. Spectrosc.*, **19**, 131 (1999).
6. T. Hirschfeld, in "Fourier Transform Infrared Spectroscopy: Applications to Chemical Systems", eds J.R. Ferraro and L.J. Basile, Academic Press, New York, 193, Vol. 2 (1979).
7. R. Williams, 'Spectroscopy and the Fourier Transform: an Interactive Tutorial', VCH Publishers, New York (1996).
8. P.R. Griffiths and J.A. deHaseth, 'Fourier Transform Infrared Spectroscopy', John Wiley & Sons, New York, Vol. 83 (1986).
9. P.R. Griffiths, 'Chemical Infrared Fourier Transform Spectroscopy', John Wiley & Sons, New York, Vol. 43 (1975).
10. S.F. Johnston, 'Fourier Transform Infrared: a Constantly Evolving Technology', Ellis Horwood, New York (1991).
11. M.P. Miller, *Appl. Spectrosc. Rev.*, **23**, 329 (1987).
12. C.J. Manning, in "Fourier Transform Spectroscopy: 11th International Conference", ed. J.A. de Haseth, American Institute of Physics, Woodbury, NY, 84, Vol. 430 (1998).
13. P.R. Griffiths, B.L. Hirsche and C.J. Manning, *Vib. Spectrosc.*, **19**, 165 (1999).
14. A. Rosencwaig, 'Photoacoustic and Photothermal Spectroscopy', John Wiley & Sons, New York, Vol. 57 (1980).
15. E.N. Lewis, P.J. Treado, R.C. Reeder, G.M. Story, A.E. Dowrey, C. Marcott and I.W. Levin, *Anal. Chem.*, **67**, 3377 (1995).
16. A.W. Mantz, *Appl. Spectrosc.*, **30**, 459 (1976).
17. W.M. Grim, J.A. Graham, R.M. Hammaker and W.G. Fateley, *Am. Lab.*, **16**, 22 (1984).
18. A.W. Mantz, *Appl. Opt.*, **17**, 1347 (1978).
19. A.A. Garrison, R.A. Crocombe, G. Mamantov and J.A. deHaseth, *Appl. Spectrosc.*, **34**, 399 (1980).
20. H. Weidner and R.E. Peale, *Appl. Opt.*, **35**, 2849 (1996).
21. H. Weidner and R.E. Peale, *Appl. Spectrosc.*, **51**, 1106 (1997).
22. H. Weidner and R.E. Peale, *Appl. Spectrosc.*, **52**, 587 (1998).
23. S.A. Rogers and S.R. Leone, *Appl. Spectrosc.*, **47**, 1430 (1993).
24. R.A. Loomis, J.P. Reid and S.R. Leone, *J. Chem. Phys.*, **112**, 658 (2000).
25. P.W. Seakins, E.L. Woodbridge and S.R. Leone, *J. Phys. Chem.*, **97**, 5633 (1993).
26. J. Lindner, R.A. Loonis, J.J. Klaassen and S.R. Leone, *J. Chem. Phys.*, **108**, 1944 (1998).
27. P.A. Berg and J.J. Sloan, *Rev. Sci. Instrum.*, **64**, 2508 (1993).
28. R.V. Kasza, J.G. Shapter, K. Griffiths, P.R. Norton and J.J. Sloan, *Surf. Sci.*, **321**, L239 (1994).
29. C.A. Carere, W.S. Neil and J.J. Sloan, *Appl. Opt.*, **35**, 2857 (1996).
30. H. Sakai and R.E. Murphy, *Appl. Opt.*, **17**, 1342 (1978).
31. R.A. Palmer, C.J. Manning, J.A. Rzepiela, J.M. Widder and J.L. Chao, *Appl. Spectrosc.*, **43**, 193 (1989).
32. R.A. Palmer, *Spectroscopy*, **8**, 26 (1993).
33. W. Uhmann, A. Becker, C. Taran and F. Siebert, *Appl. Spectrosc.*, **45**, 390 (1991).
34. H. Yang, M.C. Asplund, K.T. Kotz, M.J. Wilkens, H. Frei and C.B. Harris, *J. Am. Chem. Soc.*, **120**, 10 154 (1998).
35. E. Kaufmann, H. Frei and R.A. Mathies, *Chem. Phys. Lett.*, **266**, 554 (1997).
36. R. Rammelsberg, S. Boulas, H. Chorongiewski and K. Gewert, *Vib. Spectrosc.*, **19**, 143 (1999).
37. C. Rodig and F. Siebert, *Vib. Spectrosc.*, **19**, 271 (1999).
38. R.A. Crocombe, R. Curbelo, J. Leonardi and D.B. Johnson, *SPIE Proc.*, **1575**, 189 (1991).
39. R.A. Crocombe and S.V. Compton, 'The Design, Performance and Applications of a Dynamically-aligned Step-scan Interferometer', Bio-Rad Application Note, Digilab Division, Richmond, CA (1991).
40. C. Rodig and F. Siebert, in "Fourier Transform Spectroscopy: 11th International Conference", ed. J.A. de Haseth,

American Institute of Physics, Woodbury, NY, 388, Vol. 430 (1998).

41. M.S. Hutson and M.S. Braiman, *Appl. Spectrosc.*, **52**, 974 (1998).
42. K.M. Omberg, J.R. Schoonover, J.A. Treadway, R.M. Leasure, R.B. Dyer and T.J. Meyer, *J. Am. Chem. Soc.*, **119**, 7013 (1997).
43. A.K. Dioumaev and M.S. Braiman, *Photochem. Photobiol.*, **66**, 755 (1997).
44. R. Rammelsberg, B. Hessling, H. Chorongiewski and K. Gewert, *Appl. Spectrosc.*, **51**, 558 (1997).
45. H. Frei, in "Fourier Transform Spectroscopy: 11th International Conference", ed. J.A. de Haseth, American Institute of Physics, Woodbury, NY, 28, Vol. 430 (1998).
46. R.A. Palmer, S.E. Plunkett, P. Chen, J.L. Chao and T.J. Tague, *Mikrochim. Acta*, **14**(Suppl.), 603 (1997).
47. B.O. Budevska and C.J. Manning, *Appl. Spectrosc.*, **50**, 939 (1996).
48. H. Wang, R.A. Palmer and C.J. Manning, *Appl. Spectrosc.*, **51**, 1245 (1997).
49. H. Wang, R.A. Palmer, C.J. Manning and J.R. Schoonover, in "Fourier Transform Spectroscopy: 11th International Conference", ed. J.A. de Haseth, American Institute of Physics, Woodbury, NY, 555, Vol. 430 (1998).
50. J.P. Wang and M.A. El-Sayed, *Biophys. J.*, **76**, 2777 (1999).
51. M.W. George and J.J. Turner, *Coord. Chem. Rev.*, **177**, 201 (1998).
52. J.R. Schoonover, C.A. Bignozzi and T.J. Meyer, *Coord. Chem. Rev.*, **165**, 239 (1997).
53. C.A. Bignozzi, J.R. Schoonover and R.B. Dyer, *Comments Inorg. Chem.*, **18**, 77 (1996).
54. J.R. Schoonover, G.F. Strouse, K.M. Omberg and R.B. Dyer, *Comments Inorg. Chem.*, **18**, 165 (1995).
55. K. Masutani, H. Sugisawa, A. Yokota, Y. Furukawa and M. Tasumi, *Appl. Spectrosc.*, **46**, 560 (1992).
56. K. Masutani, A. Yolota, Y. Furakawa, M. Tasumi and A. Yoshizawa, *Appl. Spectrosc.*, **47**, 1370 (1993).
57. M.A. Czarnecki, N. Katayama, Y. Ozaki, M. Satoh, K. Yoshio, T. Watanabe and T. Yanagi, *Appl. Spectrosc.*, **47**, 1382 (1993).
58. A. Sakamoto, Y. Furukawa, M. Tasumi and K. Masutani, *Appl. Spectrosc.*, **47**, 1457 (1993).
59. A. Sakamoto, H. Okamoto and M. Tasumi, in "Fourier Transform Spectroscopy: 11th International Conference", ed. J.A. de Haseth, American Institute of Physics, Woodbury, NY, 439, Vol. 430 (1998).
60. G.L. Carr, *Vib. Spectrosc.*, **19**, 53 (1999).
61. C.J. Hirschmugl and G.P. Williams, *Synchrotron Radiat. News*, **8**, 10 (1995).
62. R.A. Palmer, G.D. Smith and P. Chen, *Vib. Spectrosc.*, **19**, 131 (1999).